Published in final edited form as:
Comput Med Imaging Graph. 2011 March ; 35(2): 148–154. doi:10.1016/j.compmedimag.2010.09.009.

CONCENTRIC DECILE SEGMENTATION OF WHITE AND HYPOPIGMENTED AREAS IN DERMOSCOPY IMAGES OF SKIN LESIONS ALLOWS DISCRIMINATION OF MALIGNANT MELANOMA

Ankur Dalal,
Department of Electrical and Computer Engineering Missouri University of Science and Technology 127 Emerson Electric Company Hall 301 West 16th Street Rolla, MO 65409-0040 Telephone: 573-341-4506 Fax: 573-341-4532 addgf3@mst.edu

Randy H. Moss, PhD,
Department of Electrical and Computer Engineering Missouri University of Science and Technology 226 Emerson Electric Company Hall 301 West 16th Street Rolla, MO 65409-0040 Telephone: 573-341-4518 Fax: 573-341-4532 rhm@mst.edu

R. Joe Stanley, PhD,
Department of Electrical and Computer Engineering Missouri University of Science and Technology 127 Emerson Electric Company Hall 301 West 16th Street Rolla, MO 65409-0040 Telephone: 573-341-6896 Fax: 573-341-4532 stanleyj@mst.edu

William V. Stoecker, MS, MD,
Stoecker & Associates 1702 E. 10th Street Rolla, MO 65401 Tel: 573-364-0122 Fax: 573-364-0129 wvs@mst.edu

Kapil Gupta, PhD,
Department of Electrical and Computer Engineering Missouri University of Science and Technology 5620 W. 133rd Terrace, Apt. 611 Overland Park, KS 66209 Telephone: 573-202-0713 Fax: 913-397-8282 kapilgupta.umr@gmail.com

David A. Calcara, B.S.,
Stoecker & Associates 1702 E. 10th Street Rolla, MO 65401 Tel: 573-364-0122 Fax: 573-364-0129 dcalcara@gmail.com

Jin Xu, B.S.,
Stoecker & Associates 1702 E. 10th Street Rolla, MO 65401 Tel: 573-364-0122 Fax: 573-364-0129 jinxu1@gmail.com

Bijaya Shrestha, PhD,
Department of Electrical and Computer Engineering Missouri University of Science and Technology 215 Emerson Electric Company Hall 301 West 16th Street Rolla, MO 65409-0040 Telephone: 573-341-6068 Fax: 573-341-4532 shrestha@mst.edu

All correspondence should be sent to: Department of Electrical and Computer Engineering Missouri University of Science and Technology 226 Emerson Electric Company Hall 301 West 16th Street Rolla, MO 65409-0040 Telephone: 573-341-4518 Fax: 573-341-4532 rhm@mst.edu .

Rhett Drugge, MD,
Sheard & Drugge MD PC 50 Glenbrook Rd. Unit 1C Stamford, CT 06902 Telephone: 203-324-5719 Fax: 203-323-7485 rhett.drugge@snet.net

Joseph M. Malters, M.D., and
The Dermatology Center 1702 E. 10th Street Rolla, MO 65401 Tel: 573-364-0122 Fax: 573-364-0129 jmalt@fidnet.com

Lindall A. Perry, M.D.
Columbia Dermatology 401 Keene Street Columbia, MO, 65201 Tel: 573-874-3300 Fax: 573-876-1678 columbiadermatology@yahoo.com

Abstract

Dermoscopy, also known as dermatoscopy or epiluminescence microscopy (ELM), permits visualization of features of pigmented melanocytic neoplasms that are not discernable by examination with the naked eye. White areas, prominent in early malignant melanoma and melanoma in situ, contribute to early detection of these lesions.

An adaptive detection method has been investigated to identify white and hypopigmented areas based on lesion histogram statistics. Using the Euclidean distance transform, the lesion is segmented in concentric deciles. Overlays of the white areas on the lesion deciles are determined. Calculated features of automatically detected white areas include lesion decile ratios, normalized number of white areas, absolute and relative size of largest white area, relative size of all white areas, and white area eccentricity, dispersion, and irregularity.

Using a back-propagation neural network, the white area statistics yield over 95% diagnostic accuracy of melanomas from benign nevi. White and hypopigmented areas in melanomas tend to be central or paracentral. The four most powerful features on multivariate analysis are lesion decile ratios.

Automatic detection of white and hypopigmented areas in melanoma can be accomplished using lesion statistics. A neural network can achieve good discrimination of melanomas from benign nevi using these areas. Lesion decile ratios are useful white area features.

Keywords

Dermoscopy; white area; regression; image analysis; melanoma; dysplastic nevi

I. INTRODUCTION

Invasive and in-situ malignant melanoma together have an incidence that, among all cancers, is one of the most rapidly increasing. Invasive melanoma alone has an estimated incidence of 58,720 and an estimated total of 8,650 deaths in the United States in 2009. [1] Contact non-polarized dermoscopy, an in-vivo skin imaging technique that uses optical magnification and liquid immersion to make subsurface lesion features visible, can detect structures known as white areas within melanomas. [2,3] As early as 1994, Stolz et. al. noted the importance of these white areas in melanoma diagnosis: “the color white is counted because the structureless area is lighter than surrounding skin, indicating regressive scar-like structures.” [4]

Figure 1 shows white areas in dermoscopy images of an amelanotic melanoma [4] (1a) and a dysplastic nevus (1b). The white areas in the melanoma have an eccentric location and an irregular shape. The white area in the nevus is located in the lesion periphery. The purpose

of this research is to discriminate melanomas from benign nevi by automatically detecting white areas and measuring features of these white areas.

II. METHODS

A. Overview

A training set of images was used to optimize white area thresholds to detect white areas. The two main steps are shown in Figure 2—lesion color segmentation, and lesion decile mask overlay.

B. Images

Two hundred forty-four benign and malignant DermLite (3Gen, Dana Point, CA) contact dermoscopy images with white areas were selected from dermoscopy images of lesions obtained from four private-practice clinics in Columbia, MO, Plantation, FL, Rolla, MO, and Stamford, CT. Fifty-seven of the dermoscopy images were of malignant melanoma: 27 in-situ melanomas and 30 invasive melanomas with a median Breslow thickness of 0.30 mm. The 57 melanomas with white areas were taken from a total of 107 melanomas, for a white area prevalence of 53.2%. All melanomas had dermatopathologist biopsy confirmation. The 187 benign lesions were nevocellular nevi. Of these 187 benign lesions, those not clearly benign on clinical and dermoscopic examination were either biopsied or were monitored and determined to have no change. The set was considered to have high diagnostic difficulty. All patients signed an informed consent form for this research, approved by the Phelps County Regional Medical Center Institutional Review Board, Rolla Missouri. Usual clinical practice was followed by all participating physicians for all lesions.

C. Lesion Color Segmentation: Optimized Adaptive White Area Detection

Thresholds for determination of white areas are determined for each color plane based on the following color histogram analysis performed on the training set of images. White areas always have a brightness that is greater than the lesion average. The goal is to find an optimal, adaptive, color segmentation for white areas, depending only upon the average and standard deviation of the pixel intensity in each color plane for any given lesion.

The white areas for the training set, 75 randomly-chosen images (25 melanomas, 50 benign) were manually marked by a student (jx) and modified as needed by a dermatologist (wvs). The marked white areas were all no darker than surrounding skin. The white areas included some hypopigmented areas (Figure 1). Image processing was performed using MATLAB (The Mathworks, 3 Apple Hill Drive, Natick, MA).

To find adaptive color thresholds, we first determined the lowest brightness threshold that identified a certain portion of the manually-marked white areas in all melanomas in the training set. Using the training set, brightness thresholds corresponding to the top (brightest) 10%, 20%, 30% and 40% of the area of the manually marked white areas were compared for all three color plane histograms. Fig. 3 shows these first-stage thresholds t_R, t_G, and t_B corresponding to 20% of the marked area along with the 10-40% range that was examined. Let the average value of a given color plane (R, G, or B) of the lesion area be labeled μ and the standard deviation of that area be σ. The difference between the threshold t and the lesion average μ in each plane may be expressed as a fraction γ of the standard deviation σ of lesion pixels in a given plane: $t - \mu = \gamma \sigma$. This same procedure is used on all three color planes to find the value of γ for each plane that corresponds to 20% of the marked white area.

For a given pixel to be considered part of the white area, all three thresholds must be met. We varied each component γ_i, i=1,2,3 in a small range centered at the 20% value described above using the training set of 75 lesions to determine the values that best found the manually-marked white areas on the 75 lesions, where "best" was determined by manually viewing the results and picking the values of the γ_i that found the largest part of the marked areas without finding much false positive area. The decision on the final value of gamma was made based on manual inspection with input from a dermatologist because it is difficult to say how much false-positive area is acceptable.

D. Two-Plane Lesion Color Segmentation to Reduce False Positive White Areas

It was found that using the above procedure on only the blue and green planes (removing the red threshold and finding new blue and green thresholds using the above procedure on two channels) reduced the number of false positive white areas. The threshold values of the blue and green planes in two-plane thresholding are higher (fewer pixels found per color, but only two planes as AND operands) than the threshold values used for the same colors in three-color-plane thresholding. The results for two- and three-color-plane thresholding are compared with the manually marked areas in Fig. 4. Removing either the blue or the green color plane threshold and thus using only one plane did not improve results, so these two thresholds were retained.

E. Lesion Decile Mask

The lesion with automatically segmented white areas is overlaid with a mask with ten approximately equal concentric areas. The Euclidean distance transform [5] is applied iteratively, accumulating pixels inward from the border pixels until thresholds of 10%, 20%, … 100% of lesion area **A** pixels are reached or exceeded. The threshold for the outer boundary of the n^{th} decile is given by $(11-n)\mathbf{A}/10$, where n= 1, 2,…10. Decile divisions are not exactly equal. A decile pixel count threshold is usually reached during a circumferential pass before a distance transform increase, but the decile is not marked until the next distance transform increase. Lesion deciles are shown in Figure 2.

F. Lesion Decile Ratios

Using binary masks, the white areas found by the two-plane optimized threshold $\mathbf{T_{BGopt}}$ are overlaid on the decile masks and the ratio R_n of white area $\mathbf{W}_n$ in the n^{th} decile to the total area in the n^{th} decile $\mathbf{A}_n$ is computed for each decile: $R_n = \mathbf{W}_n/\mathbf{A}_n$, n = 1,2,…10. The ratios of decile pairs R_i/R_j are termed lesion decile ratios. There are 90 total lesion decile ratios. Since decile areas are nearly equal, differing only by a number of pixels within a distance transform unit, shown as circumferential lines in Figure 2, $R_i/R_j \approx \mathbf{W}_i/\mathbf{W}_j$, the ratio of the white areas in the i^{th} and j^{th} deciles.

G. White Area Indices

Nine indices were examined to characterize the automatically detected white areas $\mathbf{W_i}$ in a lesion of area **A**. The first six indices are identical to those previously developed to characterize automatically detected blotches (structureless areas) in melanomas. [6] The nine white area indices are:

1. Average eccentrictity of white areas: $\mathbf{E}=\frac{\mathbf{D}}{\sqrt{\mathbf{A}}}$, where **D** is the Euclidean distance between the global white area centroid and the lesion centroid.

2. Relative size of white areas: $\mathbf{W_{rel}} = (1/\mathbf{A}) \sum_{\mathbf{i}=1}^{\mathbf{n}} \mathbf{W_i}$, where *n* is the number of white areas and $\mathbf{W_i}$ is the area of the i^{th} white area.

3. Relative size of largest white area: $\mathbf{W_{rel\text{-}max}} = \max\{i\}\mathbf{W_i} / \mathbf{A}$.

4. Absolute size of largest white area: $\mathbf{W_{max}} = \max\{i\}\mathbf{W_i}$.

5. Number of white areas normalized by lesion size: $\bar{\mathbf{n}} = \mathbf{n}/\mathbf{A}$.

6. Average border irregularity of all white areas: $\bar{\mathbf{I}} = \sum_{\mathbf{i}=1}^{\mathbf{n}} \frac{\mathbf{P_i}}{\mathbf{n}\sqrt{\mathbf{W_i}}}$, where $\mathbf{P_i}$ is the perimeter and $\mathbf{W_i}$ is the area of the i^{th} white area within the lesion.

7. First white area dispersement index, $\bar{\mathbf{DI}}(1) = \sum_{\mathbf{i}=1}^{\mathbf{n}} \frac{\mathbf{DLC_i}}{\mathbf{n}\sqrt{\mathbf{A}}}$, where $\mathbf{DLC_i}$ is the distance of the i^{th} white area centroid from the lesion centroid and **n** is the number of white areas.

8. Second white area dispersement index, $\bar{\mathbf{DI}}(2) = \sum_{\mathbf{i}=1}^{\mathbf{n}} \frac{\mathbf{DWC_i}}{\mathbf{n}\sqrt{\mathbf{A}}}$, where $\mathbf{DWC_i}$ is the distance of the i^{th} white area centroid from the global white area centroid.

9. Ratio of largest white area in the lesion, $\mathbf{W_{max}}$, to the largest white area present in the outermost decile, $\mathbf{W_{decile\ 1}} : \mathbf{L} = \mathbf{W_{max}} / \mathbf{W_{decile\ 1}}$.

The first six features were chosen because they were effective in characterizing dark blotches. [6] The last three features were selected because we suspected those features might be different in malignant melanomas and benign lesions.

H. Selection of Features

The 90 decile area ratios R*i*/R*j* and nine white area indices **E**, $\mathbf{W_{rel}}$, $\mathbf{W_{rel\text{-}max}}$, $\mathbf{W_{max}}$, $\bar{\mathbf{n}}$, $\bar{\mathbf{I}}$, $\bar{\mathbf{DI}}(1)$, $\bar{\mathbf{DI}}(2)$ and **L** were determined after using the two-color-plane method to automatically segment the white areas on the 75 training images. These image features were then analyzed using the Proc Logistic and Proc Discrim functions of SAS Statistical Analysis Software, (SAS Corp., Cary, North Carolina) to determine the best inputs to the neural network classifier.

1. Variable selection using stepwise logistic regression using Proc Logistic: The selection parameter is specified as ‘stepwise’ in the proc logistic procedure to facilitate selection of variables. The best True vs. False classification of TP = 0.90 and TN = 0.80 is observed when the following variables are selected, where the first decile is outermost and the 10^{th} decile is innermost and *RiRj* denotes the ratio of the decile percentage of the i^{th} decile to the j^{th} decile: R_5R_3, $R_{10}R_1$, R_2R_6, R_7R_6, $\bar{\mathbf{n}}$, R_4R_8, R_4R_9, R_7R_5, R_5R_9, $\bar{\mathbf{DI}}(1)$, $R_{10}R_3$, $R_{10}R_8$.

2. Linear discriminant analysis using Proc Discrim: This step is used to produce a classification table (confusion matrix). The initial inputs to the Discrim procedure are the variables obtained from the stepwise selection procedure. The final set of variables provided the highest true positive/true negative classification rates in the classification table. The highest True vs False classification of TP = 0.92 and TN = 0.86 is obtained using the same 12 features as in Proc Logistic above. (All work reported in this section dealing with feature selection and all results reported here are for the training set of 75 images.)

I. Neural Network Testing

The methods developed using the randomly selected training set of 75 lesions were applied to a test set (all remaining lesions in our overall set) of 169 lesions (137 benign nevi and 32 melanomas). In order to avoid distortion of the outer decile features in situations where the entire lesion area is not captured completely within the image, the 169-lesion data set only included lesions completely contained within the image. All lesions had manually drawn borders and automatically detected white areas, with the 12 computed features selected by SAS. Lesion discrimination was performed using combinations of the 12 features based on SAS ranking of those features. Discrimination was performed on the highest SAS ranked feature, top two ranked features, and so on up to and including all 12 features. Based on the feature combinations with number of features F, a standard back-propagation neural network with an architecture of FxF/2x1 (F input nodes, F/2 (rounded) nodes in a single hidden layer, 1 output node) was used with neural network training up to 30 epochs based on momentum of 0.9, learning rate of 0.01, and convergence with RMS error < 0.1. A leave-one-out methodology was used for training/testing because of the relatively small set of melanomas. Sigmoid transfer functions, at the input and hidden layers, and a linear transfer function, at the output, were implemented. The neural network was run on two separate cases: two-color-plane criteria before and after removing the lesions not touching the image border.

III. RESULTS

Using the two-color-plane threshold and the selected features added in the order chosen by the SAS procedures above, classification results were determined on the test set (Table 1).

IV. DISCUSSION

In the past, the term “scar-like depigmentation” has been used to describe white areas. Scar-like depigmentation was considered, along with granularity [2,7], to be a “regression structure.” In order to avoid confusion with the histopathological meaning of the term “regression,” most authors recently have employed descriptive terminology for these areas: white areas [8,9] and granularity. [7] In the international consensus conference on dermoscopy, scar-like depigmentation was defined as “areas of white distinct irregular extensions (true scarring), which should not be confused with hypo-or depigmentation due to simple loss of melanin.” [2] Hypopigmentation is a common finding in both nevi and melanoma, with an odds ratio of only 2.0, lower than the odds ratio of 5.4 for the presence of “regression structures,” i.e. white areas and granularity. [2] White areas must also be distinguished from blue-white veils. In recent years, our clinical experience, has not found blue-white veils to be common in the earlier melanomas we are observing.

Zalaudek et al. found that the presence of white areas alone could not distinguish between a group of benign nevi and a group of equivocal lesions (for which at least one pathologist diagnosed melanoma but not all pathologists diagnosed melanoma). However, the presence of both white and blue areas in combination was able to distinguish between the benign and equivocal lesions. [8] Salopek et. al. found that white and blue colors were highly specific indicators in distinguishing melanoma from benign nevi. [10] Seidenari et. al. found that of six colors studied, only black, white, and dark brown showed significant area differences between melanomas and two benign groups: Clark nevi and melanocytic nevi without atypia. [9] White areas in melanomas were more unbalanced, more compact, more asymmetric, and more centrally located than the white areas in benign lesions. [10]

In our study, we found white areas in 53.2% of melanomas in dermoscopy images, a significantly higher percentage than Seidenari et. al. noted previously (24%). The Seidenari study and our study were conducted on different populations with different imaging and

lighting techniques, and are not strictly comparable. The high incidence of white areas in our study is consistent with our inclusion of some areas of hypopigmentation within both our manually and automatically detected white areas, such as the periphery of the benign lesion in Figure 1b. This more general definition of white areas may be useful in automatic melanoma detection. Our study confirmed the importance of centrally located white areas, as the two features with the greatest significance on Proc Logistic multivariance analysis were the ratios R_5R_3 and $R_{10}R_1$. The second ratio, $R_{10}R_{1,,}$ is a measure of how central the white areas are, as it measures the ratio of the white area in the inner (tenth) decile to the white area in the outer (first) decile. In our study, these ratios were statistically of greater significance than the measures of white area compactness, size, or eccentricity.

This study lacks automatic border determination (segmentation), which can be performed using automated methods. [11] .The border accuracy varies depending upon the metric used, and is generally within range of inter-observer variation. The study test set is of limited size, with only 32 melanomas and 137 benign nevi represented.

V. FUTURE WORK

Future studies should explore additional techniques. Although our technique is a novel approach that allows successful thresholding for a wide variety of lesions, both benign and malignant, existing thresholding methods such as Otsu's could be tried. The Otsu method [12], which finds the threshold that mimimizes intraclass variances, is quite useful when separating subsets with distinct histogram characteristics. Other features, more rigorous feature selection methods, and more sophisticated pattern classifiers could be examined.

VI. CONCLUSIONS

The results of the present study confirm that white areas can assist in automatic discrimination of melanoma from benign lesions. Our definition of white areas on a lesion histogram percentile basis is chosen to automatically detect some white areas in all melanomas with white areas. We found no absolute threshold that performed as well as this adaptive threshold, which included many white areas in benign lesions. Decile overlays allow ratios of white areas found in different concentric regions of the lesion. Our study has determined that the most significant features in melanoma detection are lesion decile ratios which provide measures of the centrality of the white areas.

Acknowledgments

Funding/Support: This publication was made possible by Grant Number SBIR R44 CA-101639-02A2 of the National Institutes of Health (NIH).

Role of the Sponsor: The contents of this article are solely the responsibility of the authors and do not necessarily represent the official views of NIH, the sponsor. The sponsor had no role in the design and conduct of the study; in the collection; analysis, and interpretation of data; or in the preparation, review, or approval of the manuscript.

References

[1]. Jemal A, Siegel R, Ward E, Hao Y, Xu J, Thun MJ. Cancer statistics, 2009. CA Cancer J Clin. 2009; 59(4):225–49. [PubMed: 19474385]

[2]. Argenziano G, Soyer HP, Chimenti S, et al. Dermoscopy of pigmented skin lesions: results of a consensus meeting via the Internet. J Am Acad Dermatol. 2003; 48(5):679–93. [PubMed: 12734496]

[3]. Argenziano, G.; Soyer, HP.; De Giorgi, V.; Piccolo, D.; Carli, P.; Delfino, M., et al. Interactive Atlas of Dermoscopy. EDRA Medical Publishing; Milan Italy: 2000.

[4]. Stolz, W.; Braun-Falco, O.; Bilek, P.; Landthaler, M.; Cognetta, A. Color Atlas of Dermatoscopy. 1st ed. Blackwell Science; Oxford, UK: 2002. p. 79

[5]. Breu H, Gil J, Kirkpatrick D, Werman M. Linear time Euclidean distance transform algorithms. IEEE Transactions on Pattern Analysis and Machine Intelligence. 1995; 17(5):529–533.

[6]. Stoecker WV, Gupta K, Stanley RJ, Moss RH, Shrestha B. Detection of asymmetric blotches (asymmetric structureless areas) in dermoscopy images of malignant melanoma using relative color. Skin Res Technol. 2005; 11(3):179–84. [PubMed: 15998328]

[7]. Braun RP, Gaide O, Oliviero M, Kopf AW, French LE, Saurat JH, Rabinovitz HS. The significance of multiple blue-grey dots (granularity) for the dermoscopic diagnosis of melanoma. Br J Dermatol. 2007; 157:907. [PubMed: 17725673]

[8]. Zalaudek I, Argenziano G, Ferrara G, Soyer HP, et al. Clinically equivocal melanocytic skin lesions with features of regression: a dermoscopic-pathological study. Br J Dermatol. 2004; 150(1):64–71. [PubMed: 14746618]

[9]. Seidenari S, Pellacani G, Grana C. Colors in atypical nevi: a computer description reproducing clinical assessment. Skin Res Technol. 2005; 11(1):36–41. [PubMed: 15691257]

[10]. Salopek TG, Kopf AW, Stefanato CM, Vossaert K, Silverman M, Yadav S. Differentiation of atypical moles (dysplastic nevi) from early melanomas by dermoscopy. Dermatol Clin. 2001; 19(2):337–45. [PubMed: 11556242]

[11]. Celebi ME, Iyatomi H, Schaefer G, Stoecker WV. Lesion border detection in dermoscopy images. Comput Med Imaging Graph. 2009; 33(2):148–153. [PubMed: 19121917]

[12]. Otsu N. A Threshold Selection Method from Gray Level Histograms. IEEE Trans. on Systems, Man and Cybernetics. 1979; 9(1):62–66.

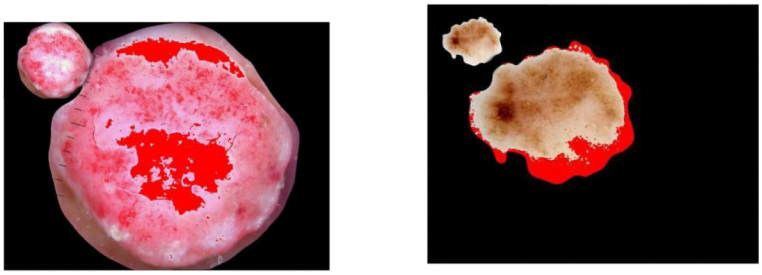

Fig. 1.
(a) White areas detected in amelanotic melanoma. Original lesion shown in inset. **(b)** White areas detected in dysplastic nevus. Original lesion shown in inset.

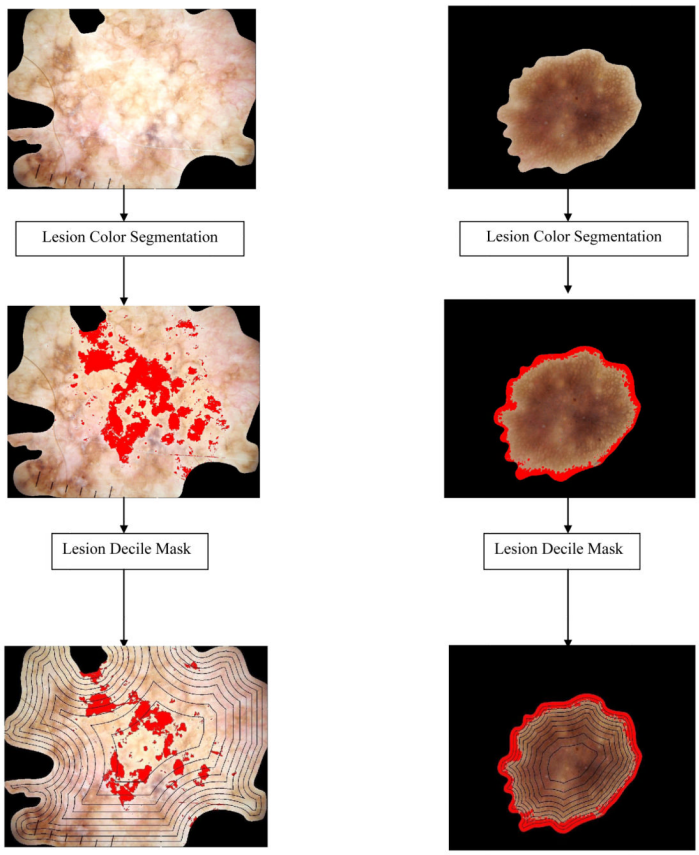

Fig. 2.
(a) Algorithm overview, melanoma. **(b)** Algorithm overview, nevus.

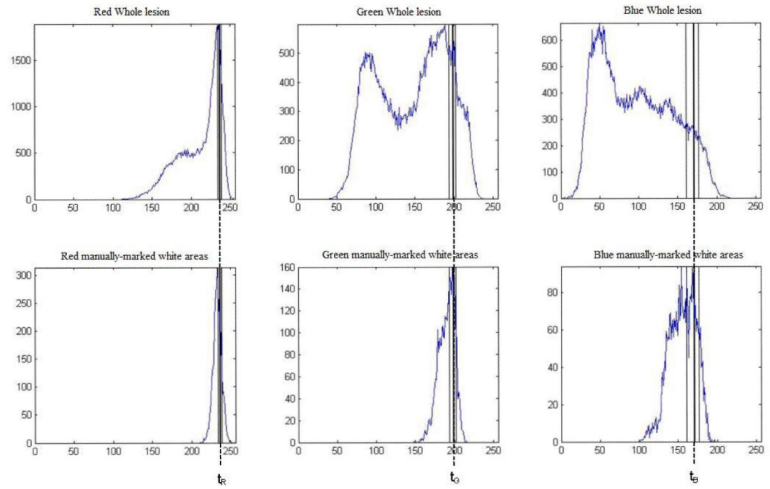

Fig. 3.

RGB histograms of a representative lesion image for the entire lesion and the manually-marked white areas with brightness threshold limits corresponding to 10% and 40% of the marked white areas. The chosen thresholds are t_R, t_G, and t_B corresponding to 20% of the marked white area. The horizontal axis in all cases is brightness in the given plane (R, G, or B) and the vertical axis is number of pixels at that brightness level.

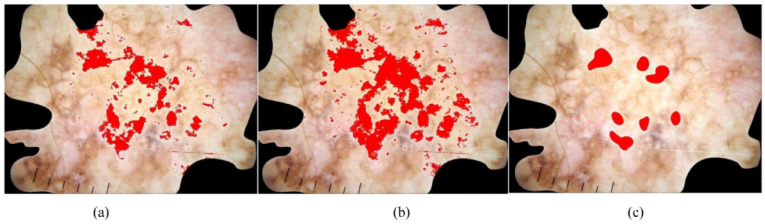

Fig. 4.
Comparison of (a) two-plane and (b) three-plane thresholding with (c) manually marked white areas

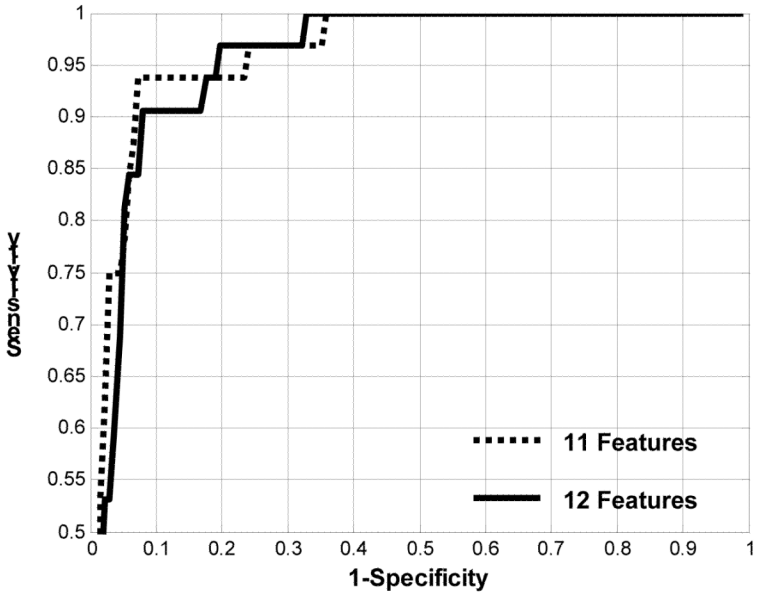

Fig. 5.
ROC curves of the entire test set for twelve features (solid line) and of the lesions not touching image edge for eleven features (dashed line).

Table1

Neural network result for 169 test lesions for two color plane criteria with lesions not touching the image edge.

Feature Combination: Features are chosen by Logistic Proc	Area Under ROC Curve (AUC)
R_5R_3	0.854
Above + $R_{10}R_1$	0.890
Above +, R_2R_6	0.936
Above + R_7R_6	0.899
Above + $\bar{\mathbf{n}}$	0.916
Above + R_4R_8	0.909
Above + R_4R_9	0.903
Above + R_7R_5	0.934
Above + R_5R_9	0.936
Above + $\bar{\mathbf{DI}}(1)$	0.943
Above + $R_{10}R_3$	0.957
Above + $R_{10}R_8$	0.952

The area under the Receiver Operating Characteristic (ROC) curve represents the diagnostic accuracy of the algorithm. Figure 5 displays ROC curves of the test set of images for the 11 (given below) and 12 feature combinations. The highest AUC results obtained was 0.957 for the 11-feature combination R_5R_3, $R_{10}R^1$, R_2R_6, R_7R_6, $\bar{\mathbf{n}}$, R_4R_8, R_4R_9, R_7R_5, R_5R_9, $\bar{\mathbf{DI}}(1)$, $R_{10}R_3$, which was close to the AUC of 0.952 for all 12 features. Overall, the results show that the decile features contribute to successful lesion discrimination, with R_5R_3 yielding an AUC of 0.854.